

## Proximity of the Protein Moiety of a GPI-Anchored Protein to the Membrane Surface: A FRET Study<sup>†</sup>

Marty T. Lehto and Frances J. Sharom\*

Guelph-Waterloo Centre for Graduate Work in Chemistry and Biochemistry, Department of Chemistry and Biochemistry, University of Guelph, Guelph, Ontario, Canada N1G 2W1

Received November 8, 2001

**ABSTRACT:** GPI-anchored proteins are ubiquitous on the eukaryotic cell surface, where they are involved in a variety of functions ranging from adhesion to enzymatic catalysis. Indirect evidence suggests that the GPI anchor may hold the protein close to the plasma membrane; however, there is a lack of direct information on the proximity of the protein portion of GPI-anchored proteins to the bilayer surface. The present study uses fluorescence resonance energy transfer (FRET) to address this important problem. The GPI-anchored ectoenzyme placental alkaline phosphatase (PLAP) was purified from a plasma membrane extract of human placental microsomes without the use of butanol. The protein was fluorescently labeled at the N-terminus with 7-(dimethylamino)coumarin-4-acetic acid succinimidyl ester (DMACA-SE) or Oregon Green 488 succinimidyl ester (OG488-SE), and each was reconstituted by detergent dilution into defined lipid bilayer vesicles containing an increasing mole fraction of a fluorescent lipid probe. The fluorescence of the labeled PLAP donors was quenched in a concentration-dependent manner by the lipid acceptors. The energy transfer data were analyzed using an approach that describes FRET between a uniform distribution of donors and acceptors in an infinite plane. The distance of closest approach between the protein moiety of PLAP and the lipid–water interfacial region of the bilayer was estimated to be smaller than 10–14 Å. This indicates that the protein portion of PLAP is located very close to the lipid bilayer, possibly resting on the surface. This contact may allow transmission of structural changes from the membrane surface to the protein, which could influence the behavior and catalytic properties of GPI-anchored proteins.

A wide variety of proteins are anchored to the external surface of the eukaryotic plasma membrane via a glycosylphosphatidylinositol (GPI)<sup>1</sup> anchor (1–4). This group of proteins includes extracellular coat proteins (such as the variant surface of *Trypanosoma* species), adhesion proteins (for example, LFA-3), surface antigens (lymphocyte Thy-1), receptors (for example, the folate receptor), and many hydrolytic ectoenzymes, including 5'-nucleotidase (5'-NTase), acetylcholinesterase, dipeptidase, and alkaline phosphatase. GPI-anchored proteins have been identified in all eukaryotic cell types, from yeast and protozoa to higher plants and mammals (5).

Although there seems to be no common functional relevance among proteins that use the GPI anchor as a means of membrane insertion, the anchor itself appears to confer some important properties on proteins to which it is attached. These include release by endogenous and exogenous bacterial phospholipases C and D (6–9), which gives rise to soluble forms of the protein lacking the GPI anchor in the circulation. The GPI anchor also acts to target proteins to the apical surface of polarized cells (10) and often leads to rapid lateral mobility in the plasma membrane (11). The presence of the GPI anchor also directs proteins to be sequestered in lipid rafts, which are sphingolipid- and cholesterol-rich microdomains proposed to exist in the plasma membrane of eukaryotic cells (12, 13). Raft microdomains are characterized by their insolubility in cold nonionic detergents such as Triton X-100 (14) and are thought to exist in the liquid-ordered state (15), a phase that is intermediate between the solid gel phase and the fluid liquid-crystalline phase. Interactions between sphingolipids and cholesterol and the long saturated acyl chains typically found in GPI anchors are thought to be responsible for their localization in lipid rafts (16). In recent years, lipid rafts have been implicated in a number of important cellular processes, including signal transduction (17–19), budding of enveloped viruses (20, 21), and bacteria–host cell interactions (22).

There is little information on the proximity of the protein portion of GPI-anchored proteins to the surface of the cell.

<sup>†</sup> This work was supported by a grant to F.J.S. from the Natural Sciences and Engineering Research Council of Canada.

\* To whom correspondence should be addressed. Telephone: (519) 824-4120 ext 2247. Fax: (519) 766-1499. E-mail: sharom@chembio.uoguelph.ca.

<sup>1</sup> Abbreviations: CHAPS, 3-[(3-cholamidopropyl)dimethylammonio]-1-propanesulfonate; C<sub>18</sub>RhoB, octadecyl rhodamine B; DMACA-SE, 7-(dimethylamino)coumarin-4-acetic acid succinimidyl ester; DMPC, dimyristoylphosphatidylcholine; DOPC, dioleoylphosphatidylcholine; FRET, fluorescence resonance energy transfer; GPI, glycosylphosphatidylinositol; Hepes, *N*-(2-hydroxyethyl)piperazine-*N'*-2-ethanesulfonic acid; MB-PE, Marina Blue–phosphatidylethanolamine; MES, 2-(*N*-morpholino)ethanesulfonic acid; NBD-PE, 7-(nitrobenz-2-oxa-1,3-diazol-4-yl)-1,2-dihexadecanoyl-*sn*-glycero-3-phosphoethanolamine; 5'-NTase, 5'-nucleotidase; OG488-SE, Oregon Green 488 succinimidyl ester; PC, phosphatidylcholine; PE, phosphatidylethanolamine; PLAP, placental alkaline phosphatase; PNP, *p*-nitrophenyl phosphate.

However, biochemical and modeling studies have suggested that they may be close to each other. Studies in our laboratory (23) and that of others (24) have suggested that the protein portion of the GPI-anchored ectoenzyme 5'-NTase may be in direct contact with the membrane bilayer. This was suggested on the basis of the fact that the enzyme exhibited a discontinuity in the Arrhenius plot when the bilayer was converted from the solid gel phase to the fluid liquid-crystalline phase (23). In addition, the glycan portion of the GPI anchor of Thy-1 was predicted to lie either between the lipid surface and the protein in a tightly folded conformation (25) or in a carbohydrate-binding pocket within the protein itself (26). In both models, the protein domain of Thy-1 is visualized as being very close to, or in contact with, the bilayer. Measurement of the distance between the protein portion of GPI-anchored proteins and the bilayer surface, using a biophysical approach, would aid in the elucidation of the nature of the association of this class of proteins with the membrane.

FRET has become a powerful biophysical technique since it was first proposed as a "spectroscopic ruler" for measuring distances in biological systems (27). The technique has been used to measure inter- and intramolecular distances in proteins and the distance between a defined site in a protein and the membrane surface. For the integral membrane transport protein, the Ca<sup>2+</sup>-ATPase, FRET was used to estimate the distance of the Ca<sup>2+</sup> and ATP binding sites from the membrane surface (28, 29), the location of an active site lysine residue relative to several probes within the bilayer (30), and the distances between several cysteine residues and the active site lysine (31). FRET also determined that the  $\alpha$ ,  $\beta$ , and  $\gamma$  subunits of heterotrimeric G-protein were located close to the bilayer (32), whereas the binding site in the growth hormone receptor was distant from the bilayer (33). More recently, FRET was used to elucidate the proximity of the active sites of the two nucleotide-binding domains of the P-glycoprotein multidrug transporter to the membrane surface (34) and to each other (35).

The present study describes the application of FRET to measure the proximity of the protein portion of the GPI-anchored ectoenzyme, human placental alkaline phosphatase (PLAP), to the membrane surface. Using a purified, reconstituted system, the protein portion of PLAP was shown to be quite close to the bilayer, possibly resting on the membrane surface.

## MATERIALS AND METHODS

**Materials.** Egg phosphatidylethanolamine (PE) and egg phosphatidylcholine (PC) were supplied by Avanti Polar Lipids (Alabaster, AL). 3-[(3-Cholamidopropyl)dimethylammonio]-1-propanesulfonate (CHAPS), L-histidyl-diazobenzylphosphonic acid (phosphonate)-agarose, *p*-nitrophenyl phosphate (PNP), ethylaminoethanol, and Triton X-114 were purchased from Sigma Chemical Co. (St. Louis, MO). Extracti-Gel D detergent removing gel was purchased from Pierce Chemical Co. (Rockford, IL). Con A-Sepharose was purchased from Amersham Pharmacia Biotech AB (Baie D'Urfé, Quebec, Canada). Marina Blue-1,2-dihexadecanoyl-*sn*-glycero-3-phosphoethanolamine (MB-PE), 7-(dimethylamino)coumarin-4-acetic acid succinimidyl ester (DMACA-SE), octadecyl rhodamine B chloride (C<sub>18</sub>RhoB), (7-nitro-

benz-2-oxa-1,3-diazol-4-yl)-1,2-dihexadecanoyl-*sn*-glycero-3-phosphoethanolamine (NBD-PE; triethylammonium salt), and Oregon Green 488 succinimidyl ester (OG488-SE) were purchased from Molecular Probes (Eugene, OR).

**Purification of PLAP.** PLAP was purified from human placenta by a modification of the method of Hawrylak (36). Human placenta was obtained within 1 h of delivery and immediately placed on ice. The umbilical cord and connective tissue were removed, and the remaining tissue was rinsed in cold phosphate-buffered saline to remove most of the blood, divided into ~100 g portions, and flash frozen in liquid nitrogen until ready for purification. Thawed placenta (100 g) was combined with 100 mL of homogenization buffer (50 mM Tris-HCl/1 mM MgCl<sub>2</sub>/0.1 mM ZnCl<sub>2</sub>, pH 8.5), together with two tablets of a protease inhibitor cocktail (Pierce, Rockford, IL). The mixture was homogenized in a Waring blender for 3 min on low speed followed by 3 min on high speed. The homogenized sample was passed through two layers of cheesecloth to remove large debris and then divided into two equal volumes. Plasma membrane vesicles were prepared from each half according to the method of Maeda et al. (37). Briefly, homogenized placenta (50 g) was layered over a sucrose cushion (41% w/v), followed by ultracentrifugation at 95000g. Plasma membrane was solubilized in 50 mM CHAPS (final protein concentration 1.5 mg/mL) for 4 h at 4 °C, followed by ultracentrifugation at 38000g for 30 min. The aqueous layer was recovered and chromatographed on a Con A-Sepharose column equilibrated with basic column buffer (BCB; 20 mM Tris-HCl/0.5 M NaCl/1 mM MgCl<sub>2</sub>/1 mM CaCl<sub>2</sub>, and protease inhibitors as above, pH 8.5). The pH of the pooled enzyme fractions (eluted with 0.4 M methyl  $\alpha$ -D-glucoside in BCB) was adjusted to 6.0 by the addition of 100 mM 2-(*N*-morpholino)ethanesulfonic acid (MES), pH 5.0, and enzyme was then adsorbed to phosphonate-agarose and eluted with 50 mM PNP in MES buffer (pH 6.0). The PLAP-active fractions were combined, dialyzed extensively against 10 mM ammonium bicarbonate buffer (pH 7.4), lyophilized to dryness, and stored at -70 °C.

**Assay for PLAP Activity.** PLAP activity was assayed in 96-well plates in 1.0 M ethylaminoethanol/1.5 mM MgCl<sub>2</sub> (pH 9.8) containing 10 mM PNP at 37 °C. The absorbance at 404 nm was monitored using a 96-well kinetic plate reader, and enzyme activity was reported as PNP released (micromoles per minute per milligram).

**Absorption Spectra and Fluorescence Excitation/Emission Spectra.** Absorption spectra were recorded using a Perkin-Elmer Lambda 6 UV-visible spectrophotometer (Perkin-Elmer, Norwalk, CT) with both sample and reference cells at 22 °C. Fluorescence spectra were recorded on a PTI Alphascan-2 spectrofluorometer (Photon Technology International, London, Ontario, Canada) with the cell holders thermostated at 22 °C. The excitation and emission slit widths were both set at 4 nm.

**Fluorescent Labeling of PLAP.** PLAP was labeled with DMACA-SE and OG488-SE on the basis of the protocol outlined by the manufacturer of the fluorescent dyes (Molecular Probes, Eugene, OR). Pure lyophilized PLAP was resuspended in 20 mM PBS containing 0.1% Triton X-100 (pH 6.5). The pH of the buffer was selected to label specifically the N-terminal amino acid residue of PLAP by reducing the reactivity of lysine side chain residues. The dye

in DMSO was added to PLAP (dye:protein mole ratio = 20:1), and the sample was stirred at room temperature for 4 h. The reaction was terminated by the addition of 50 mM hydroxylamine ( $1/40$  of the volume) and stirred for an additional 30 min at room temperature. Following chromatographic separation on a Sephadex G-25 column or a Micro Bio-spin column (Bio-Rad Laboratories, Mississauga, Ontario, Canada), the labeled protein was further purified by three rounds of Triton X-114 phase separation. The detergent phase was diluted 10-fold in 50 mM Tris-HCl/0.15 M NaCl/0.25 M sucrose (pH 7.5), and Triton X-114 was removed by chromatography on an Extract-Gel D column equilibrated with the same buffer. The purified, fluorescently labeled protein (DMACA-PLAP or OG488-PLAP) was made up to 2 mM CHAPS using 200 mM CHAPS in 50 mM Tris-HCl/0.15 M NaCl/0.25 M sucrose (pH 7.5) and stored at  $-70^{\circ}\text{C}$ .

**Removal of the GPI Anchor from DMACA-PLAP and OG488-PLAP.** The GPI anchor was removed from the two types of labeled PLAP using HF, as described (38, 39). Briefly, PLAP (20–100  $\mu\text{g}$  of protein in 20  $\mu\text{L}$  of buffer) was incubated on ice in a microfuge tube with 50  $\mu\text{L}$  of ice-cold HF for 16 h in the dark. The residual HF was removed using a SpeedVac, and the resulting pellet was resuspended in 20  $\mu\text{L}$  of nonreducing Laemmli's buffer for SDS-PAGE analysis.

**Preparation of Reconstituted Vesicles Containing PLAP.** DMACA-PLAP and OG488-PLAP were reconstituted into phospholipid vesicles by a detergent dilution method. Egg PC, egg PE, DOPC, NBD-PE, and  $\text{C}_{18}\text{RhoB}$  were stored at  $-20^{\circ}\text{C}$  in  $\text{CH}_3\text{Cl}/\text{MeOH}$  (2:1 v/v). DMACA-PLAP was reconstituted into 1:1 (mole ratio) egg PC/egg PE vesicles containing increasing mole fractions of NBD-PE, whereas OG488-PLAP was reconstituted into DOPC vesicles containing increasing mole fractions of  $\text{C}_{18}\text{RhoB}$ . Egg PC (0.15  $\mu\text{mol}$ ) and a mixture of egg PE and the appropriate amount of NBD-PE (total PE + NBD-PE of 0.15  $\mu\text{mol}$ ) were dispensed into a series of microfuge tubes. DOPC (0.3  $\mu\text{mol}$ ) and the appropriate amount of  $\text{C}_{18}\text{RhoB}$  were treated in the same manner. The lipid mixtures were dried under a gentle stream of nitrogen and then further dried in a vacuum desiccator for 1 h. To the dried lipid was added 10  $\mu\text{L}$  of 25 mM CHAPS/0.25 M sucrose in 50 mM Tris-HCl buffer (pH 7.4), and the contents were vortexed and sonicated in a Sonogen sonicator (Branson Instruments, Inc., Stamford, CT) at  $37^{\circ}\text{C}$ . The mixture was chilled on ice, and DMACA-PLAP or OG488-PLAP (6 mg in 30  $\mu\text{L}$  of 2 mM CHAPS in 0.25 M sucrose/Tris-HCl buffer) was added. After incubation on ice for 30 min, the volume of each sample was then diluted to 1 mL with 0.25 M sucrose/Tris-HCl buffer, and the resulting vesicles were resuspended with a fine-gauge needle. The final lipid and protein concentrations were 0.3 mM and 6  $\mu\text{g}/\text{mL}$ , respectively, with a lipid:protein ratio of 50:1 (w/w). Control vesicles were prepared in the same manner using unlabeled PLAP.

**Dynamic Light Scattering.** The size profile of the reconstituted vesicles was determined using dynamic light scattering (DLS). This technique involves the measurement of the scattering of light at  $90^{\circ}$  to the incident of a laser beam directed at a sample of freely diffusing vesicles. Fluctuations in the intensity of the scattered light generate an autocorrelation function that is directly related to the diffusion

coefficient,  $D$ , of the vesicles in solution. The radius of the vesicles was calculated from  $D$  using the Stokes–Einstein equation, assuming spherical, hollow particles.

**Fluorescent Labeling and Reconstitution of Thy-1.** Thy-1 antigen was purified from rat brain as described previously (40) and labeled at the N-terminus with DMACA by the same technique as that used for PLAP (see above). The labeled protein was reconstituted into bilayer vesicles of 1:1 (mole ratio) egg PC/egg PE containing NBD-PE by dilution, as described for labeled PLAP.

**Resonance Energy Transfer Measurements.** Fluorescence intensities were measured using a PTI Alphascan-2 spectrofluorometer (Photon Technology International, London, Ontario, Canada). The excitation wavelengths for DMACA-PLAP and OG488-PLAP were 377 and 495 nm, respectively, while emission was measured at 469 and 525 nm, respectively, with 4 nm slits. Fluorescence intensities were corrected for light scattering using controls containing unlabeled PLAP, and the inner filter effect was corrected at both the excitation and emission wavelengths using the equation (41–43):

$$F_{\text{icor}} = (F_i - B)10^{0.5b(A_{\lambda_{\text{ex}}} + A_{\lambda_{\text{em}}})} \quad (1)$$

where  $F_{\text{icor}}$  is the corrected value of the fluorescence intensity,  $F_i$  is the experimentally measured fluorescence intensity,  $B$  is the background fluorescence intensity,  $b$  is the path length in centimeters, and  $A_{\lambda_{\text{ex}}}$  and  $A_{\lambda_{\text{em}}}$  are the absorbances of the sample at the excitation and emission wavelengths, respectively. For the OG488 fluorophore, the excitation and scans of the dye were essentially superimposable when run in buffer, or in buffer containing the lipid vesicles, so that the portion of the inner filter effect correction relating to light scattering was very small. For the DMACA fluorophore, there was a very small effect on fluorescence emission of light scattering by the vesicles, but the overall inner filter correction to the fluorescence values was small, in the range of 5–10%.

**Determination of Parameters for FRET Analysis.** The resonance energy transfer efficiency ( $E$ ) between donor and acceptor can be written as

$$E = 1 - F/F_0 \quad (2)$$

where  $F$  and  $F_0$  are the fluorescence intensities of the donor in the presence and absence of the acceptor, respectively. FRET efficiency is related to the distance ( $R$ ) between the donor and acceptor by the equation:

$$R = R_0(E^{-1} - 1)^{1/6} \quad (3)$$

where  $R_0$  is the distance at which the efficiency of energy transfer is 50%.  $R_0$  is calculated from

$$R_0 = (9.8 \times 10^3)(J\kappa^2Q_Dn^{-4})^{1/6} (\text{\AA}) \quad (4)$$

where  $J$  is the spectral overlap integral between donor and acceptor in units of  $\text{cm}^3 \text{M}^{-1}$ ,  $\kappa^2$  is the orientation factor [taken as  $2/3$  based on the assumption that donor and acceptor dipoles are mobile (44)],  $Q_D$  is the fluorescence quantum yield of the donor, and  $n$  is the refractive index of the medium between the chromophores which, for a dilute aqueous solution, is equal to 1.33 (45).

The spectral overlap integral,  $J$ , is defined by

$$J = \frac{\int F_D(\lambda)\epsilon_A(\lambda)\lambda d\lambda}{\int F_D(\lambda)d\lambda} \quad (5)$$

where  $F_D(\lambda)$  and  $\epsilon_A(\lambda)$  are the donor emission and the acceptor molar extinction coefficients, respectively, at  $\lambda$ . The fluorescence emission spectra of DMACA-PLAP and OG488-PLAP were recorded using excitation at 377 and 495 nm, respectively, and the absorption spectra of NBD-PE and C<sub>18</sub>RhoB were measured. The spectral data were used to calculate  $J$  using eq 5 with the aid of a computer program designed by Dr. Uwe Oehler (Department of Chemistry and Biochemistry, University of Guelph).

The quantum yields,  $Q_D$ , of DMACA-PLAP and OG488-PLAP in reconstituted vesicles were determined relative to standards, using polarizers set to 0° in the excitation beam and 54.7° (magic angle) in the emission beam. The fluorescence emission spectrum of DMACA-PLAP was compared to the emission spectrum of a standard solution of quinine sulfate in 0.1 N H<sub>2</sub>SO<sub>4</sub> (both sample and standard had the same absorbance of <0.1 at 377 nm).  $Q_{\text{DMACA-PLAP}}$  was calculated using the equation:

$$Q_{\text{DMACA-PLAP}} = \frac{F_{\text{DMACA-PLAP}}}{F_{\text{quinine}}} Q_{\text{quinine}} \quad (6)$$

where  $Q_{\text{quinine}}$  is 0.51 in 0.1 N H<sub>2</sub>SO<sub>4</sub> (46) and  $F_{\text{DMACA-PLAP}}$  and  $F_{\text{quinine}}$  are the integrals of the fluorescence of DMACA-PLAP and quinine sulfate in the wavelength range 385–675 nm, respectively. The quantum yield of OG488-PLAP was calculated in the same manner, using fluorescein in 0.1 N NaOH as the standard with  $Q_{\text{fluorescein}}$  equal to 0.91 (46), over an integral wavelength range of 505–700 nm (excitation at 495 nm). Background scattering was corrected with reconstituted vesicles containing unlabeled PLAP at the same protein concentration.

*Analysis of the Distance between Donor and Acceptor.* Since the distance of closest approach ( $L$ ) between the donor and the acceptor in the FRET experiments was much less than  $R_0$ , the data were analyzed using the analytical approach derived by Wolber and Hudson (47). The solution calculates the distance of closest approach between a uniform population of randomly distributed donors and acceptors on an infinite plane and is described by a simple series approximation:

$$F/F_0 = A_1 e^{-k_1 c} + A_2 e^{-k_2 c} \quad (7)$$

where

$$C = cR_0^2 \quad (8)$$

The parameter  $c$  describes the surface density of acceptors measured in number per Å<sup>2</sup>. The value of  $c$  was calculated by dividing the mole ratio of acceptor/membrane lipids by the average area of the headgroups of phospholipids, 80 Å<sup>2</sup> (42). The values of  $A_1$ ,  $k_1$ ,  $A_2$ , and  $k_2$  were taken from the tables of the exact solution to the series approximation by Wolber and Hudson for different ratios of  $L/R_0$  (47).

## RESULTS

*Purification of PLAP.* Human PLAP was successfully purified using a two-step affinity chromatography procedure,

Table 1: Purification of PLAP from Human Placenta<sup>a</sup>

stage of purification	protein	total activity (mg)	specific activity (units × 10 <sup>-3</sup> )	x-fold purification (units/mg)
plasma membrane	144 ± 1	70.5 ± 14.9	0.49 ± 0.11	1
CHAPS extract	112 ± 2	404 ± 61	3.61 ± 0.17	7
Con A column eluate	*	*	*	
phosphonate column eluate	3.3 ± 0.1	48.1 ± 3.4	14.7 ± 1.6	30

<sup>a</sup> Samples from various stages of the purification procedure were assayed for PLAP activity as described in Materials and Methods. One unit of activity corresponds to 1 μmol of PNP hydrolyzed/min at 37 °C, pH 9.8. Data are presented as the mean ± SEM ( $n = 3$ ). The presence of sugar interferes with the protein assay and enzyme activity in the Con A column eluate (\*), so that values cannot be determined accurately.

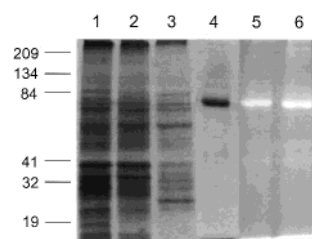


FIGURE 1: Purification of PLAP from human placenta. The plasma membrane preparation from human placenta (lane 1, 10 μg of protein), CHAPS-solubilized placental plasma membrane (lane 2, 10 μg), the glycoprotein fraction (lane 3, 10 μg), and purified PLAP (lane 4, 8 μg) were subjected to SDS-PAGE analysis in a 10% (w/v) polyacrylamide gel, followed by staining with silver. OG488-PLAP (lane 5, 10 μg) were electrophoresed in a 10% (w/v) polyacrylamide gel, viewed on a trans-illuminator, and the fluorescent bands were photographed with black and white Kodak film. The position of the molecular mass markers is indicated on the left. OG488-PLAP (lane 6, 10 μg) after removal of the GPI anchor using HF (see Materials and Methods).

first on Con A-Sepharose (which isolates α-D-mannose-containing glycoproteins) and then on agarose conjugated to a covalently bound nonhydrolyzable substrate analogue, phosphonate (Table 1). The plasma membrane starting material was treated with the zwitterionic detergent CHAPS, which was able to solubilize ~80% of the total membrane-bound protein from the lymphocyte plasma membrane. After purification on the Con A and phosphonate columns, a 30-fold purification was obtained relative to the plasma membrane starting material. SDS-PAGE analysis of highly purified PLAP resulted in a major band with an apparent  $M_r$  of ~74 kDa (Figure 1, lane 4).

In this work, PLAP was purified from the plasma membrane fraction isolated from placental microsomes (Figure 1, lane 1). This method was adopted to eliminate the butanol extraction procedure that is commonly used as a first step in alkaline phosphatase purification (48). Triton X-114 phase partitioning revealed that >95% of PLAP isolated by this method partitioned into the detergent phase, indicating that it had retained a GPI anchor (data not shown). Thus, isolation of the placental plasma membrane as a first step resulted in a fraction that contained almost exclusively GPI-anchored PLAP, as compared to butanol extraction, which can isolate non-GPI-anchored PLAP depending on the pH of the extraction (49). Also, the placental plasma

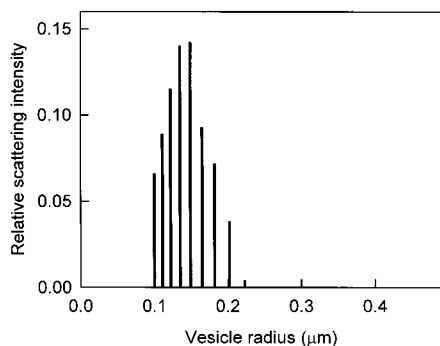


FIGURE 2: Size distribution of reconstituted vesicles containing PLAP. Lipid bilayer vesicles composed of egg PC/egg PE (1:1 mole ratio) containing PLAP were prepared by detergent dilution using CHAPS. The lipid to protein ratio was 50:1 (w/w) ( $\sim$ 650:1 mole ratio). DLS measurement of the vesicle size distribution was carried out as described in Materials and Methods.

membrane fraction provides a starting material that is substantially more enriched in PLAP than a butanol extract, as can be seen by the fact that only a 30-fold enrichment from plasma membrane was needed to achieve homogeneous PLAP in this study (Table 1), compared to the  $\sim$ 500–1000-fold enrichment required from the butanol extraction in other reports (49, 50).

**Fluorescent Labeling and Reconstitution of PLAP.** PLAP was specifically labeled on the amino group of the N-terminal amino acid residue by adjusting the pH of the labeling reaction to 6.5, which has the effect of protonating Lys residues (and thus reducing their activity) while leaving the N-terminus partially deprotonated. The results of SDS-PAGE analysis of the labeled protein showed a single highly fluorescent band for OG488-PLAP (Figure 1, lane 5) and DMACA-PLAP (not shown). The GPI anchor also includes moieties with free amino functional groups, such as glucosamine and phosphoethanolamine. To check that the fluorescent label was covalently linked to the protein portion of PLAP, rather than one of these components, the GPI anchor was removed from DMACA-PLAP and OG488-PLAP using chemical treatment with HF. Both species of fluorescently labeled PLAP showed a small shift in mobility on SDS-PAGE after HF treatment, comparable to that reported by others (38, 39), indicating that the GPI anchor had been removed. The fluorescent label was clearly retained after HF treatment (see Figure 1, lane 6, for OG488-PLAP), indicating that it was linked to the protein, rather than the GPI anchor.

DMACA-PLAP and OG488-PLAP, the donors in the FRET studies, were reconstituted into lipid bilayers containing fluorescently labeled lipid acceptors. DMACA-PLAP was reconstituted into bilayers of egg PC/egg PE (1:1 mole ratio) containing NBD-PE as the acceptor, and OG488-PLAP was reconstituted into DOPC bilayers containing  $C_{18}$ RhoB as the acceptor. Both of these labeled lipids have been commonly used as FRET acceptors (33, 34, 51–53). DLS analysis of the reconstituted vesicles showed that they comprised a relatively homogeneous population of large vesicles (probably unilamellar) with a mean diameter of  $\sim$ 0.3  $\mu$ m (Figure 2).

**Resonance Energy Transfer.** To assess the relative distance between the fluorescent label on PLAP and the lipid bilayer, energy transfer must take place between the DMACA-

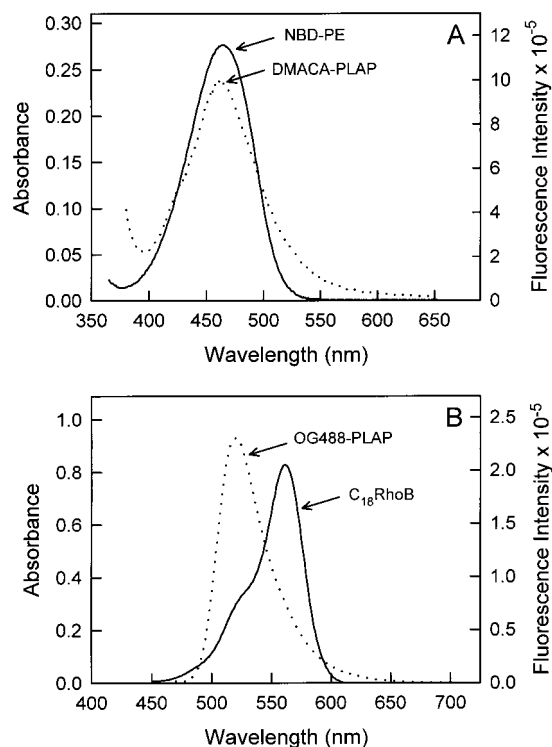


FIGURE 3: Overlap of the fluorescence emission spectra of the donors with the UV-visible absorption spectra of the acceptors. (A) Fluorescence emission spectrum of DMACA-PLAP ( $\lambda_{\text{ex}} = 345$  nm, right scale) and the UV-visible absorption spectrum of NBD-PE (left scale). (B) Fluorescence emission spectrum of OG488-PLAP ( $\lambda_{\text{ex}} = 465$  nm, right scale) and the UV-visible absorption spectrum of  $C_{18}$ RhoB (left scale).

Table 2: Spectral Parameters for Donor and Acceptor Pairs

FRET donor	FRET acceptor	donor quantum yield $Q_D$	overlap integral $J$ ( $\text{cm}^3 \text{M}^{-1}$ )	$R_0^a$ ( $\text{\AA}$ )
DMACA-PLAP	NBD-PE	0.530	$5.81 \times 10^{-14}$	39.6
OG488-PLAP	$C_{18}$ RhoB	0.513	$5.07 \times 10^{-13}$	56.5

<sup>a</sup> The refractive index,  $n$ , was taken as 1.33, and the orientation factor,  $\kappa^2$ , was assumed to be  $2/3$  (see Materials and Methods).

OG488-labeled protein donors and the fluorescent lipid acceptors in the membrane. Energy transfer requires that there be a significant amount of overlap between the fluorescence emission spectrum of the donor and the absorbance spectrum of the acceptor. Figure 3A shows the overlap of the fluorescence emission spectrum of DMACA-PLAP and the absorption spectrum of NBD-PE, and Figure 3B shows the spectral overlap of the emission spectrum of OG488-PLAP and the absorption of  $C_{18}$ RhoB. The spectral overlap for both pairs is quite large (see Table 2 for the spectral overlap integral,  $J$ ), and the value of  $R_0$  was calculated to be 39.6  $\text{\AA}$  for the DMACA-PLAP/NBD-PE combination and 56.5  $\text{\AA}$  for the OG488-PLAP/ $C_{18}$ RhoB combination. The large values of  $R_0$  indicate that these two donor-acceptor pairs are highly suitable for FRET studies. In the case of NBD-PE labeled in the headgroup, the fluorophore is known to be located in the interfacial region of the bilayer, in the vicinity of the glycerol backbone (51). The fluorescent probe on  $C_{18}$ RhoB is also known to be positioned in the polar headgroup region of the bilayer (Molecular Probes, Eugene, OR).

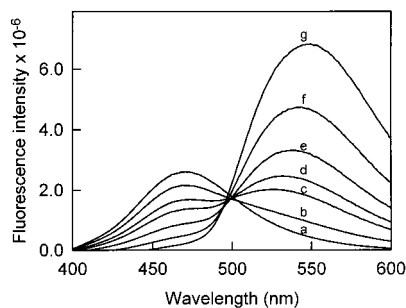


FIGURE 4: Fluorescence resonance energy transfer between a PLAP donor and lipid acceptors. Proteoliposomes of egg PC/egg PE (1:1 mole ratio) contained DMACA-PLAP and increasing mole fractions of the lipid acceptor NBD-PE: (a) 0, (b) 0.001, (c) 0.005, (d) 0.0075, (e) 0.015, (f) 0.025, and (g) 0.05. The ratio of total phospholipid:PLAP was 50:1 (w/w) (~650:1 mole ratio). Emission bandwidths were 4 nm.

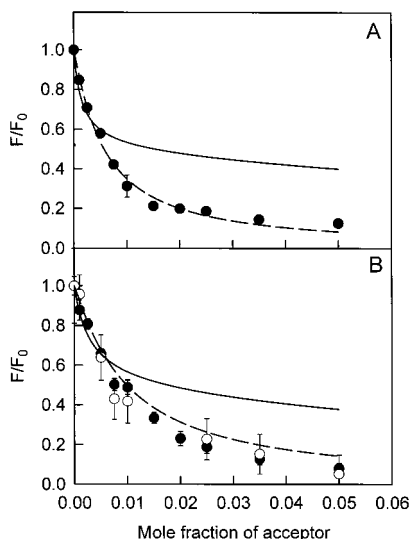


FIGURE 5: Fitting of FRET data from the donor–acceptor pairs to the models of Dewey and Hammes and Koppel et al. (A) Fitting of the FRET data for OG488-PLAP and  $C_{18}$ RhoB (●) to the models of Dewey and Hammes (—) and Koppel et al. (---). (B) Fitting of the FRET data for DMACA-PLAP and NBD-PE (●) to the models of Dewey and Hammes (—) and Koppel et al. (---). For the Koppel fitting, the radius of the vesicles was taken as 150 nm (see Figure 2). The Koppel fitting indicated values of  $L$  of 15.8 and 5.34 Å for (A) and (B), respectively. Data for energy transfer between MB-PE and NBD-PE included in the same bilayer are also shown (○). Data points represent the mean  $\pm$  SEM ( $n = 3$ ). Where error bars are not visible, they are contained within the symbols.

Figure 4 shows a progressive decrease in the fluorescence emission of DMACA-PLAP, and a corresponding increase in the sensitized fluorescence emission of NBD-PE, when the protein was reconstituted into vesicles with increasing mole fractions of NBD-PE and excited at the excitation wavelength of the donor (377 nm). Similarly, the fluorescence emission of OG488-PLAP decreased in the presence of increasing mole fractions of  $C_{18}$ RhoB in the bilayer, accompanied by sensitized fluorescence emission by  $C_{18}$ RhoB upon excitation at 490 nm, the excitation wavelength of the donor. Clearly, energy transfer is occurring between the donor fluorophore on the protein and the acceptor fluorophore in the lipid bilayer. The results of the quenching of donors are summarized in Figure 5, which shows the relative fluorescence of the donor with respect to the mole ratio of acceptor. The fluorescence emission of both OG488-PLAP

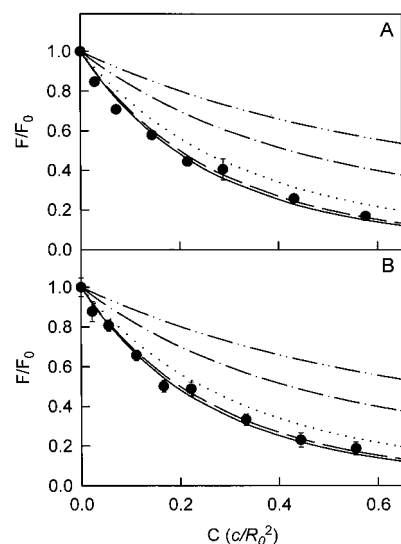


FIGURE 6: Analysis of the FRET data from the donor–acceptor pairs for PLAP. (A) Analysis of the FRET data for OG488-PLAP and  $C_{18}$ RhoB according to the approximation of Wolber and Hudson (see Materials and Methods) where  $L = 0$  Å (—),  $L = 14.1$  Å (---),  $L = 28.3$  Å (···),  $L = 45.2$  Å (— · —), and  $L = 56.5$  Å (— · · —). (B) Fitting of the FRET data for DMACA-PLAP and NBD-PE where  $L = 0$  Å (—),  $L = 9.9$  Å (---),  $L = 19.8$  Å (···),  $L = 31.6$  Å (— · —), and  $L = 39.6$  Å (— · · —). Data points represent the mean  $\pm$  SEM ( $n = 3$ ). Where error bars are not visible, they are contained within the symbols.

and DMACA-PLAP was efficiently quenched with increasing mole fractions of the acceptors. This quenching can be seen to be highly efficient by comparing it to the quenching curves determined for the situation where the donor and acceptor are both lipids coreconstituted in the same bilayer, MB-PE and NBD-PE (Figure 5B, open circles). The high efficiency of quenching indicates that the donor and acceptor are in close proximity, such that the ratio of the distance of closest approach,  $L$ , to the value of  $R_0$  is small, i.e.,  $L/R_0 \rightarrow 0$ . Initially, we attempted to fit the data to the models of Dewey and Hammes (54) and Koppel et al. (55). The experimental data could not be fitted to the Dewey and Hammes model (Figure 5), which assumes that donors and acceptors are distributed on parallel planes separated by a distance  $h$ . The data set for DMACA-PLAP and NBD-PE fitted reasonably well to the model of Koppel et al., which assumes that the donors and acceptors lie on spherical shells of radius  $R$  and  $R + h$ , respectively ( $h$  can be thought of as equivalent to  $L$ ), resulting in a value for  $h$  of  $15.8 \pm 4.8$  Å (Figure 5A). The FRET data for OG488-PLAP and  $C_{18}$ RhoB fitted less well to the Koppel model (Figure 5B), with a value of  $h$  of  $5.34 \pm 187$  Å, the large error indicating that the fit was poor. Thus the Koppel model fits gave an indication that the donor and acceptor were located relatively close together, at a distance much less than  $R_0$ . In the situation where  $L/R_0 \rightarrow 0$ , the data can be fitted to a simple series approximation derived by Wolber and Hudson (47), which describes energy transfer between a uniform distribution of donors and acceptors on an infinite plane (see Materials and Methods). With this approximation,  $F/F_0$  depends only on the acceptor surface density ( $c$ ) and  $R_0$ ; it does not depend on  $L$ . In Figure 6, the FRET data were fitted to the exact solutions derived by Wolber and Hudson (47) for values of  $L/R_0$ . In Figure 6A, the quenching of OG488-PLAP by  $C_{18}$ RhoB is shown to fit quite well to values of  $L$  between

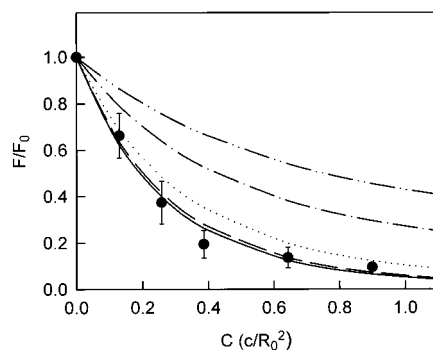


FIGURE 7: Analysis of the FRET data from the donor–acceptor pair for reconstituted Thy-1. The FRET data for DMACA-Thy-1 and NBD-PE were analyzed according to the approximation of Wolber and Hudson (see Materials and Methods), where  $L = 0$  Å (—),  $L = 9.9$  Å (---),  $L = 19.8$  Å (···),  $L = 31.6$  Å (— · —), and  $L = 39.6$  Å (— · · —). Data points represent the mean  $\pm$  SEM ( $n = 3$ ). Where error bars are not visible, they are contained within the symbols.

0 and 14.1 Å and does not fit when  $L$  approaches 28 Å. The data for DMACA-PLAP and NBD-PE fit to values of  $L$  between 0 and 9.9 Å but not to a value of  $L$  of 19.8 Å and larger (Figure 6B). Thus, the results obtained from both donor–acceptor pairs indicate that the fluorescent labels on PLAP are quite close to the interfacial regions of the bilayer, with a maximum distance of closest approach of  $\sim 10$ –14 Å. These results suggest that the GPI anchor is in a conformation that holds the attached protein very close to the membrane surface.

To determine whether this is also true for other proteins with GPI anchors, the GPI-anchored antigen Thy-1 was labeled at the N-terminus with DMACA and reconstituted into lipid vesicles containing NBD-PE, in exactly the same fashion as PLAP. As shown in Figure 7, the resulting FRET data (shown compared to the solutions of Wolber and Hudson) indicated that the two fluorophores were also positioned relatively close to each other. Thus this GPI-anchored protein likewise appears to be located close to the surface of the lipid bilayer.

## DISCUSSION

Little is known about the proximity of GPI-anchored proteins to the surface of the plasma membrane. One possibility is that the protein moiety of a GPI-anchored protein is located some distance from the membrane, as a result of the GPI anchor being in an extended conformation (the “lollipop” model; see Figure 8A). Alternatively, if the GPI anchor folds up into a compact conformation, or lies along the membrane surface, the protein may “flop down” onto the membrane, where its activity could be modulated by the properties of the bilayer (see Figure 8B). In the case of 5'-NTase, the catalytic properties of the enzyme are affected by the phase state and fluidity of the bilayer, strongly suggesting that it may contact the membrane (23, 24).

Our approach in the present study was to use resonance energy transfer to measure the distance between a GPI-anchored protein and the interfacial region of the bilayer. The FRET donor consisted of purified, fluorescently labeled PLAP, reconstituted into lipid bilayer vesicles containing a headgroup-labeled membrane lipid probe as the acceptor. PLAP was purified to homogeneity (see Figure 1) using a

modified procedure that eliminated the butanol extraction step commonly employed to purify the protein (48). By isolating a plasma membrane preparation as a first step in the redesigned purification procedure, a larger fraction of the contaminating proteins was eliminated when compared to the butanol extraction approach, and >95% of the final purified protein retained a GPI anchor.

For energy transfer experiments, purified PLAP labeled with DMACA or OG488 was reconstituted into lipid bilayers containing varying amounts of the labeled membrane probes NBD-PE or C<sub>18</sub>RhoB, respectively. Fluorescence measurements revealed that DMACA-PLAP/NBD-PE and OG488-PLAP/C<sub>18</sub>RhoB were highly suitable donor–acceptor pairs for FRET experiments, with a substantial degree of overlap between donor emission and acceptor absorption and high  $R_0$  values. There was a high degree of donor quenching in the presence of increasing amounts of the acceptor in both cases, indicating that the donor and acceptor were located relatively close together. The dependence of donor quenching on acceptor concentration did not fit the model of Dewey and Hammes (54), which has been used successfully to measure the distance between specific sites in various proteins and the membrane surface, including P-glycoprotein (34), the EGF receptor (33), and the Ca<sup>2+</sup>-ATPase (28, 29). In all of these cases, the estimated distances separating the donor and acceptor were quite large, on the order of (1–1.5) $R_0$ , so that acceptor mole fractions up to 0.4–0.6 were necessary for >90% quenching of the donor fluorescence. In the present study, donor quenching was almost complete at 0.05 mole fraction of the lipid acceptor (see Figure 5). The quenching data obtained in the present study could be fitted to the model of Koppel et al. (55), with a distance of closest approach of  $\sim 16$  Å for DMACA-PLAP (a relatively good fit) and  $\sim 5$  Å for OG488-PLAP (a poor fit), which gave an indication that the separation distance between the donor and acceptor was much less than  $R_0$ . The data for both donor–acceptor fluorophores fitted quite well to the series approximation of Wolber and Hudson (47), which is intended for application to cases where the separation distance is small relative to  $R_0$ . The distance of closest approach between the fluorescent label on the PLAP protein and the surface of the bilayer was estimated to be less than 10–14 Å. Distance values this small are approaching the lower limit that can be reliably measured by FRET (41). When the GPI-anchored antigen Thy-1 was labeled with DMACA and used in a similar experiment, analysis of the results according to Wolber and Hudson also indicated a small distance of closest approach. For comparison, distances of closest approach between small fluorescent lipid labels coreconstituted into the same lipid bilayer are  $\sim 10$  Å, as measured by FRET (54, 56) (see Figure 5B). Taken together, the results of the present study indicate that the protein moieties of PLAP and Thy-1 antigen are positioned very close to the bilayer, possibly resting on the membrane surface.

The X-ray crystal structure of PLAP has recently been solved at 1.8 Å resolution (PDB 1EW2; Figure 8) (57). The structure confirms the accumulated biochemical evidence that PLAP is a dimer (58) and identifies several groups of residues that may contribute to the allosteric properties of the protein. However, a large C-terminal portion, residues 480–513, and the GPI anchor that would be attached to the C-terminal Asp residue (59) are missing from the X-ray

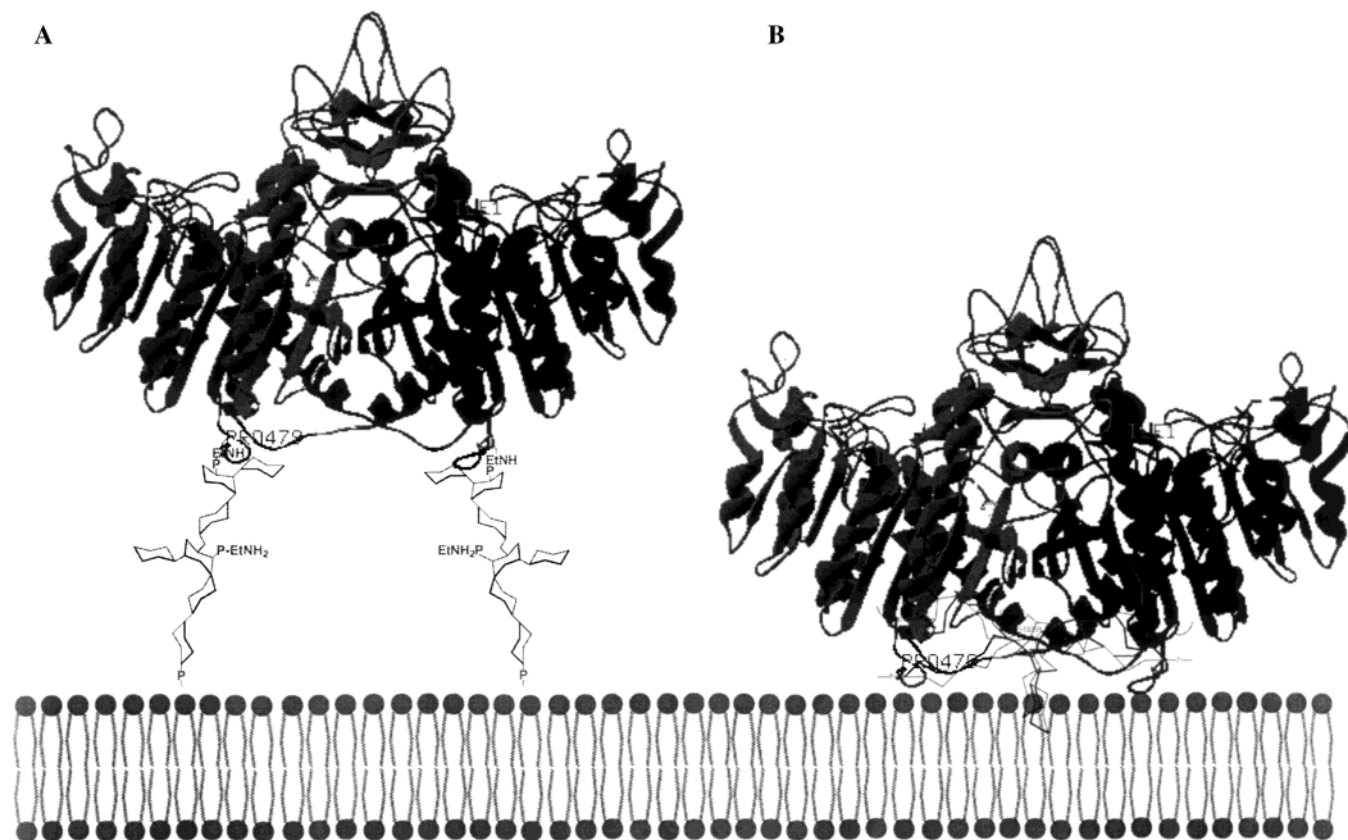


FIGURE 8: Models of dimeric PLAP in relation to the bilayer surface. (A) Model of the crystal structure of the PLAP dimer, showing the two GPI anchors in a fully extended conformation (lollipop model) with the protein moiety some distance from the membrane. (B) The protein portion of PLAP may flop down onto the membrane with the GPI anchor folded up beneath it, causing the enzyme to be in direct contact with the bilayer surface.

structural model. The inability to obtain structural data for this C-terminal region indicates that it has a high degree of flexibility. The distance between Pro479 (the last visible C-terminal residue in the crystal structure) and the N-terminal Ile is 51.5 Å (as measured by RasMol Version 2.7.1). However, the high degree of flexibility in the rather large unstructured C-terminal region would allow for a wide variation in this distance. The dimeric structure presented by Le Du et al. (57) indicates that the N-terminus of one monomer is much closer to the C-terminus of the second monomer than to the C-terminus of the same subunit (see Figure 8). The results of the current study are consistent with the PLAP dimer resting on the surface of the membrane with each monomer in close proximity to the bilayer surface.

Although the method used to label PLAP is selective for the N-terminus, it is possible that some fraction of the fluorescent label is present on the  $\epsilon$ -amino groups of internal Lys residues. However, even if this were the case, our conclusion that the protein moiety of PLAP is located close to the membrane surface would still be valid. We consider it highly unlikely that the fluorescent probes themselves might induce binding of the GPI-anchored protein to the membrane surface, but we cannot rule it out. As pointed out earlier, there is substantial independent evidence for association of GPI-anchored proteins with the membrane surface.

In previous work, we demonstrated that cleavage of the GPI anchor of 5'-NTase resulted in catalytic activation of the enzyme and showed that the degree of activation depended on the nature of the lipid bilayer into which the protein was reconstituted (60). Our laboratory also reported

that reconstituted 5'-NTase demonstrated a decrease in activation energy when the bilayer was converted from the solid gel phase to the fluid liquid-crystalline phase (23). In addition, 5'-NTase from rat enterocytes displayed a break point on Arrhenius plots, which coincided with a lipid thermotropic transition (24). Taken together, these results indicate that the protein portion of 5'-NTase may also be in direct contact with the lipid bilayer, which can modulate the catalytic properties of the enzyme. Modeling studies of the GPI-anchored lymphocyte antigen Thy-1 suggested that this may be the case for this protein as well. The glycan portion of the GPI anchor of Thy-1 is predicted to lie either between the lipid surface and the protein in a tightly folded conformation (25) or in a carbohydrate-binding pocket within the protein itself (26), and it may thus impose a particular conformation on the protein. In both models, the protein domain of Thy-1 is visualized as being very close to, or in contact with, the bilayer. The results of the present study provide experimental evidence to support this proposal.

If this is true of GPI-anchored proteins in general, there are several implications for the structure and function of this class of proteins. Such contact would provide a mechanism for transmission of structural changes from the membrane surface to the protein. First, changes in the fluidity of the membrane might modulate the catalytic properties of all GPI-anchored proteins, as has been observed for 5'-NTase (24, 60, 61). In addition, such close contact between the protein and the membrane as a result of GPI anchor insertion may affect the catalytic properties of the protein, independent of the physical properties of the membrane. We previously

reported that the turnover number of the enzyme 5'-NTase is reduced when the GPI anchor is membrane inserted, and this results in catalytic activation when the anchor is cleaved by PI-specific phospholipase C and the protein is released from the membrane surface (60). Finally, close association of the protein and its GPI anchor with the membrane may affect the ability of the phospholipase to approach and cleave the anchor. We have recently demonstrated that the kinetics of cleavage of 5'-NTase by PI-specific phospholipase C is highly modulated by the physical properties of the lipid bilayer (62), which may arise in part from the close association of the protein and its anchor with the membrane surface.

## REFERENCES

- Ferguson, M. A. J. (1999) *J. Cell Sci.* 112, 2799–2809.
- Zhou, F. X., Merianos, H. J., Brunger, A. T., and Engelman, D. M. (2001) *Proc. Natl. Acad. Sci. U.S.A.* 98, 2250–2255.
- Hooper, N. M. (1997) *Clin. Chim. Acta* 266, 3–12.
- McConville, M. J., and Ferguson, M. A. (1993) *Biochem. J.* 294, 305–324.
- Eisenhaber, B., Bork, P., and Eisenhaber, F. (2001) *Protein Eng.* 14, 17–25.
- Griffith, O. H., Volwerk, J. J., and Kuppe, A. (1991) *Methods Enzymol.* 197, 493–502.
- Huang, K. S., Li, S., and Low, M. G. (1991) *Methods Enzymol.* 197, 567–575.
- Metz, C. N., Brunner, G., Choi-Muira, N. H., Nguyen, H., Gabrilove, J., Caras, I. W., Altszuler, N., Rifkin, D. B., Wilson, E. L., and Davitz, M. A. (1994) *EMBO J.* 13, 1741–1751.
- Movahedi, S., and Hooper, N. M. (1997) *Biochem. J.* 326, 531–537.
- Lisanti, M. P., Sargiacomo, M., Graeve, L., Saltiel, A. R., and Rodriguez-Boulant, E. (1988) *Proc. Natl. Acad. Sci. U.S.A.* 85, 9557–9561.
- Noda, M., Yoon, K., Rodan, G. A., and Koppel, D. E. (1987) *J. Cell Biol.* 105, 1671–1677.
- Simons, K., and Ikonen, E. (1997) *Nature* 387, 569–572.
- Brown, D. A., and London, E. (2000) *J. Biol. Chem.* 275, 17221–17224.
- Hooper, N. M., and Turner, A. J. (1988) *Biochem. J.* 250, 865–869.
- Ahmed, S. N., Brown, D. A., and London, E. (1997) *Biochemistry* 36, 10944–10953.
- Schroeder, R., London, E., and Brown, D. A. (1994) *Proc. Natl. Acad. Sci. U.S.A.* 91, 12130–12134.
- Cary, L. A., and Cooper, J. A. (2000) *Nature* 404, 945–947.
- Czech, M. P. (2000) *Nature* 407, 147–148.
- Ilangumaran, S., He, H. T., and Hoessli, D. C. (2000) *Immunol. Today* 21, 2–7.
- Scheiffele, P., Rietveld, A., Wilk, T., and Simons, K. (1999) *J. Biol. Chem.* 274, 2038–2044.
- Nguyen, D. H., and Hildreth, J. E. K. (2000) *J. Virol.* 74, 3264–3272.
- Shin, J. S., Gao, Z. M., and Abraham, S. N. (1999) *Biosci. Rep.* 19, 421–432.
- Sharom, F. J., Lorimer, I., and Lamb, M. P. (1985) *Can. J. Biochem. Cell Biol.* 63, 1049–1057.
- Brasitus, T. A., and Schachter, D. (1980) *Biochemistry* 19, 2763–2769.
- Barboni, E., Rivero, B. P., George, A. J., Martin, S. R., Renoup, D. V., Hounsell, E. F., Barber, P. C., and Morris, R. J. (1995) *J. Cell Sci.* 108, 487–497.
- Rademacher, T. W., Edge, C. J., and Dwek, R. A. (1991) *Glycobiology* 1, 41–42.
- Stryer, L. (1978) *Annu. Rev. Biochem.* 47, 819–846.
- Gutierrez-Merino, C., Munkonge, F., Mata, A. M., East, J. M., Levinson, B. L., Napier, R. M., and Lee, A. G. (1987) *Biochim. Biophys. Acta* 897, 207–216.
- Munkonge, F., East, J. M., and Lee, A. G. (1989) *Biochim. Biophys. Acta* 979, 113–120.
- Teruel, J. A., and Gomez-Fernandez, J. C. (1987) *Biochem. Int.* 14, 409–416.
- Gomez-Fernandez, J. C., Corbalan-Garcia, S., Villalain, J., and Teruel, J. A. (1994) *Biochem. Soc. Trans.* 22, 826–829.
- Remmers, A. E., and Neubig, R. R. (1993) *Biochemistry* 32, 2409–2414.
- Carraway, K. L., Koland, J. G., and Cerione, R. A. (1990) *Biochemistry* 29, 8741–8747.
- Liu, R., and Sharom, F. J. (1998) *Biochemistry* 37, 6503–6512.
- Qu, Q., and Sharom, F. J. (2001) *Biochemistry* 40, 1413–1422.
- Hawrylak, K., Kihn, L., Rutkowski, D., and Stinson, R. A. (1990) *Clin. Chim. Acta* 186, 197–201.
- Maeda, T., Balakrishnan, K., and Mehdi, S. Q. (1983) *Biochim. Biophys. Acta* 731, 115–120.
- Butikofer, P., Boschung, M., and Menon, A. K. (1995) *Anal. Biochem.* 229, 125–132.
- Mayor, S., Menon, A. K., Cross, G. A., Ferguson, M. A., Dwek, R. A., and Rademacher, T. W. (1990) *J. Biol. Chem.* 265, 6164–6173.
- Reid-Taylor, K. L., Chu, J. W. K., and Sharom, F. J. (1999) *Biochem. Cell Biol.* 77, 189–200.
- Lakowicz, J. R. (1999) in *Principles of Fluorescence Spectroscopy*, Kluwer Academic Publishers, New York.
- Liu, R., and Sharom, F. J. (1996) *Biochemistry* 35, 11865–11873.
- Parker, C. A. (1968) in *Photoluminescence of Solutions*, Elsevier Publishing Co., Amsterdam.
- Dale, R. E., Eisinger, J., and Blumberg, W. E. (1979) *Biophys. J.* 26, 161–193.
- Wu, C. W., and Stryer, L. (1972) *Proc. Natl. Acad. Sci. U.S.A.* 69, 1104–1108.
- Goldberg, M. C. (1989) in *Luminescence applications in biological, chemical, environmental, and hydrological science*, American Chemical Society, Washington, DC.
- Wolber, P. K., and Hudson, B. S. (1979) *Biophys. J.* 28, 197–210.
- Holmgren, P. A., Stigbrand, T., Damber, M. G., and von Schoultz, B. (1979) *Obstet. Gynecol.* 54, 631–634.
- Miki, A., Tanaka, Y., Ogata, S., and Ikehara, Y. (1986) *Eur. J. Biochem.* 160, 41–48.
- Bublitz, R., Armesto, J., Hoffmann-Blume, E., Schulze, M., Rhode, H., Horn, A., Aulwurm, S., Hannappel, E., and Fischer, W. (1993) *Eur. J. Biochem.* 217, 199–207.
- Chattopadhyay, A. (1990) *Chem. Phys. Lipids* 53, 1–15.
- Mutucumarana, V. P., Duffy, E. J., Lollar, P., and Johnson, A. E. (1992) *J. Biol. Chem.* 267, 17012–17021.
- Zheng, Y., Shopes, B., Holowka, D., and Baird, B. (1991) *Biochemistry* 30, 9125–9132.
- Dewey, T. G., and Hammes, G. G. (1980) *Biophys. J.* 32, 1023–1035.
- Koppel, D. E., Fleming, P. J., and Strittmatter, P. (1979) *Biochemistry* 18, 5450–5457.
- Fung, B. K., and Stryer, L. (1978) *Biochemistry* 17, 5241–5248.
- Le Du, M. H., Stigbrand, T., Taussig, M. J., Menez, A., and Stura, E. A. (2001) *J. Biol. Chem.* 276, 9158–9165.
- Durbin, H., Tucker, D. F., Milligan, E. M., Bobrow, L. G., Warne, P. H., Pookim, Y. L., and Bodmer, W. F. (1988) *Int. J. Cancer, Suppl.* 2, 50–58.
- Redman, C. A., Thomas-Oates, J. E., Ogata, S., Ikehara, Y., and Ferguson, M. A. (1994) *Biochem. J.* 302, 861–865.
- Lehto, M. T., and Sharom, F. J. (1998) *Biochem. J.* 332, 101–109.
- Sharom, F. J., McNeil, G. L., Glover, J. R., and Seier, S. (1996) *Biochem. Cell Biol.* 74, 701–713.
- Lehto, M. T., and Sharom, F. J. (2002) *Biochemistry* 41, 1398–1408.